Graphene–Co3O4 nanocomposite as an efficient bifunctional catalyst for lithium–air batteries

ARTICLE · APRIL 2014

DOI: 10.1039/C4TA00802B

11 AUTHORS, INCLUDING:

Chunwen Sun
Chinese Academy of Sciences
61 PUBLICATIONS **2,178** CITATIONS
SEE PROFILE

Fan Li
Beijing University of Technology
39 PUBLICATIONS **275** CITATIONS
SEE PROFILE

Wei Yang
Graduate School at Shenzhen, Tsinghua Un…
14 PUBLICATIONS **180** CITATIONS
SEE PROFILE

Yujin Chen
Harbin Engineering University
127 PUBLICATIONS **4,202** CITATIONS
SEE PROFILE

Volume 2 | Number 20 | 28 May 2014 | Pages 7119–7616

Journal of Materials Chemistry A

Materials for energy and sustainability

www.rsc.org/MaterialsA

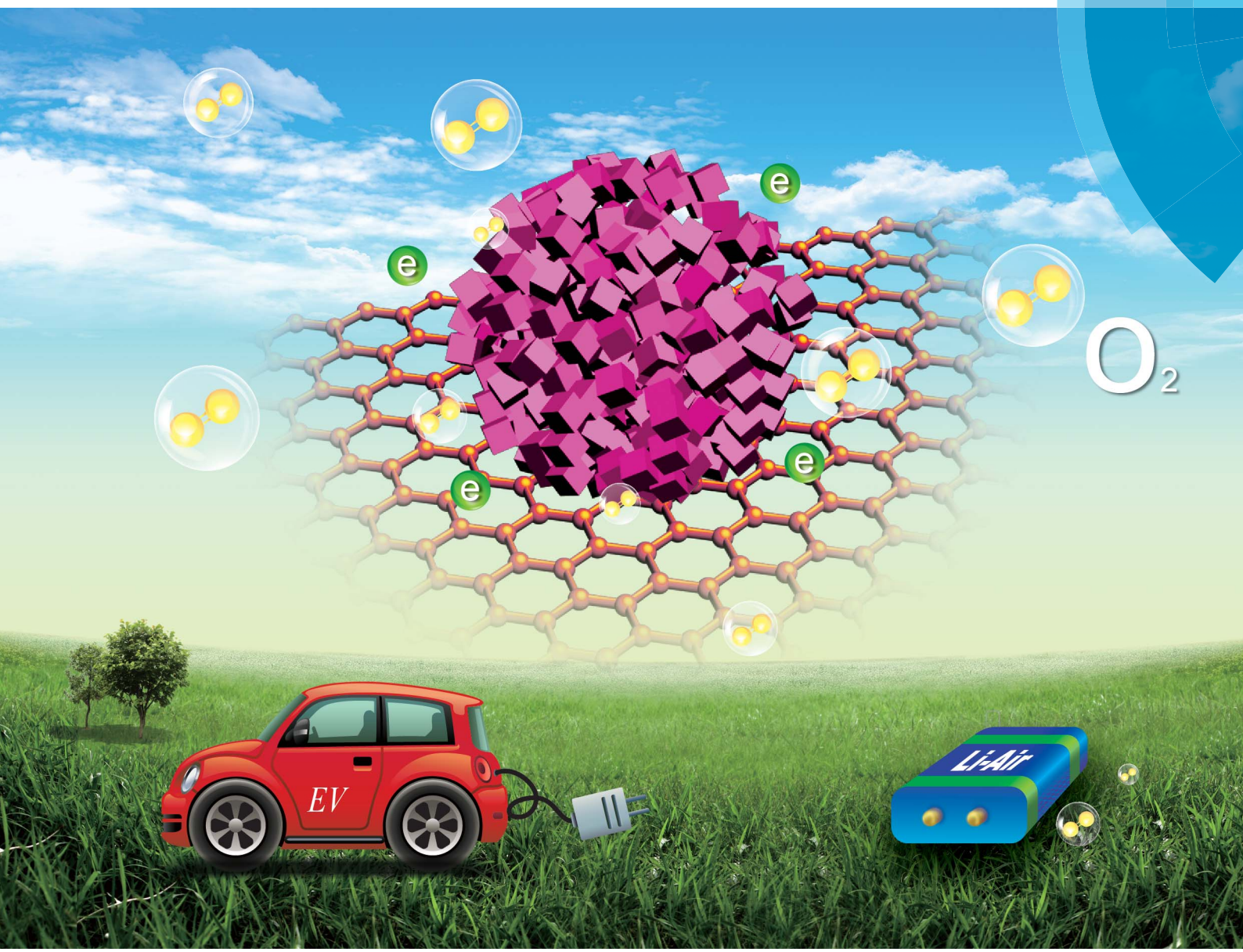

ISSN 2050-7488

ROYAL SOCIETY OF CHEMISTRY

PAPER

Chunwen Sun, Yujin Chen, Youngsik Kim *et al.*

Graphene–Co_3O_4 nanocomposite as an efficient bifunctional catalyst for lithium–air batteries

Journal of Materials Chemistry A

PAPER

Graphene–Co_3O_4 nanocomposite as an efficient bifunctional catalyst for lithium–air batteries†

Cite this: *J. Mater. Chem. A*, 2014, **2**, 7188

Chunwen Sun,*[a] Fan Li,[d] Chao Ma,[b] Yan Wang,[d] Yulan Ren,[c] Wei Yang,[a] Zhaohui Ma,[a] Jianqi Li,[b] Yujin Chen,*[c] Youngsik Kim*[e] and Liquan Chen[a]

Received 15th February 2014
Accepted 24th March 2014

DOI: 10.1039/c4ta00802b

www.rsc.org/MaterialsA

A facile hydrothermal route has been developed to prepare graphene–Co_3O_4 nanocomposites. The graphene–Co_3O_4 nanocomposite catalyst demonstrates an excellent catalytic activity toward oxygen-reduction reaction including a considerably more positive half-wave potential (−0.23 V) than that of pristine graphene (−0.39 V), as well as higher cathodic currents. More importantly, this catalyst shows better long-term durability than the commercial Pt/C catalyst in an alkaline solution. The preliminary results indicate that the graphene–Co_3O_4 nanocomposite is an efficient and stable bifunctional catalyst for Li–air batteries and may be an alternative to the high-cost commercial Pt/C catalyst for the ORR/OER in alkaline solutions.

1. Introduction

The oxygen-reduction reaction (ORR) is an important process in the energy conversion and storage in applications such as fuel cells[1,2] and metal–air batteries.[3,4] The high cost of Pt cathodes and the poor durability of proton exchange membrane (PEM) fuel cells remain the primary obstacles hindering its commercial development. Among various metal–air batteries, lithium (Li)–air batteries possess the highest theoretical gravimetric energy density (11 140 W h kg^{-1}) if oxygen is accessed directly from the air.[5] However, respective limitations in the oxygen evolution reaction (OER) and ORR during the charge and discharge processes in current rechargeable Li–air battery technology are issues that still await solution, in addition to high costs. The sluggish kinetics of the ORR and OER in Li–air batteries is ascribed to low efficiency of catalysts.[4,5] The performance of the Li–air batteries can be drastically improved by incorporating an efficient catalyst to achieve higher discharge voltage, lower charge voltage and improved rate performance.[6] Therefore, the design of a low-cost and stable bifunctional electrocatalyst is a major challenge to the construction of efficient Li–air batteries.

The cathode catalysts normally used to catalyze air reactions are carbon black or carbon loaded with a noble metal.[3] Oxidation of a carbon support in Li–air batteries should be paid more attention than that in a PEM fuel cell. Many spinel cobaltite oxides have been investigated as electrocatalysts for the ORR or OER.[7,8] Bruce *et al.* reported the screening of many catalysts that could be used in facilitating the electrochemical properties of the O_2 electrode in a non-aqueous Li–O_2 cell.[9] Among the various oxide catalysts studied, Co_3O_4 gives the best compromise between initial capacity and capacity retention as well as the lowest charging voltage of 4 V. Recently, we demonstrated that perovskite $Sr_{0.95}Ce_{0.05}CoO_{3-\delta}$ loaded with copper nanoparticles on their surface are shown to be excellent, low-cost, and stable bifunctional catalysts for oxygen-reduction and oxygen-evolution reactions in an aqueous solution.[3] Dai *et al.* reported a hybrid material consisting of Co_3O_4 nanocrystals grown on reduced graphene oxide as a high-performance bifunctional catalyst for the ORR and OER.[10] Yang *et al.* demonstrated the influence of morphology on the bifunctionality of porous Co_3O_4 microspheres for Li–air batteries.[4] Among carbon materials, graphene, a two-dimensional aromatic monolayer of sp^2-hybridized carbon atoms, has become a promising candidate for ORR catalysis due to its high conductivity and excellent mechanical properties, which are greatly favorable for the harsh ORR process.[11,12] Recently, the bifunctional composite catalysts of Co_3O_4 nanofibers immobilized on nonoxidized graphene nanoflakes have been demonstrated in Li–O_2 batteries by Ryu *et al.*[13] The mechanism of Co_3O_4/graphene catalytic activity in

[a]*Key Laboratory for Renewable Energy, Beijing Key Laboratory for New Energy Materials and Devices, Beijing National Laboratory for Condensed Matter Physics, Institute of Physics, Chinese Academy of Sciences, Beijing 100190, China. E-mail: csun@iphy.ac.cn; Fax: +86-10-82649046; Tel: +86-10-82649901*

[b]*Laboratory for Advanced Materials & Electron Microscopy, Beijing National Laboratory for Condensed Matter Physics, Institute of Physics, Chinese Academy of Sciences, Beijing 100190, China*

[c]*College of Science, Harbin Engineering University, Harbin, Heilongjiang, 150001, China. E-mail: chenyujin@hrbeu.edu.cn; Fax: +86-451-82519754; Tel: +86-451-82519754*

[d]*College of Environmental and Energy Engineering, Beijing University of Technology, Beijing 100124, China*

[e]*Interdisciplinary School of Green Energy, Ulsan National Institute of Science and Technology, Ulsan (UNIST), Ulsan, Korea. E-mail: ykim@unist.ac.kr; Fax: +82-52-217-3009; Tel: +82-52-217-2921*

† Electronic supplementary information (ESI) available. See DOI: 10.1039/c4ta00802b

Li–O_2 batteries with carbonate-based electrolytes has been studied by Lim *et al.*[14] To our knowledge, there are no reports on the systematic studies on the ORR and OER properties of graphene (G)–Co_3O_4 nanocomposites as well as its applications as bifunctional catalysts for Li–air batteries. Herein, we report highly active and stable graphene (G)–Co_3O_4 nanocomposite electrocatalysts synthesized *via* a facile hydrothermal route and subsequent thermal treatment process. The catalytic properties related to ORR and OER were investigated by means of cyclic voltammetry (CV) and linear sweep voltammograms (LSVs). As a bifunctional catalyst, a round-trip electric-energy storage efficiency of 76.5% for the graphene–Co_3O_4 catalysts was observed in the aqueous Li–air cell.

2. Experimental

Material synthesis

Graphene sheets used in this work were purchased from Nanjing XFNano Material Tech Co. Ltd, and their diameter and thickness were in the range of 0.5–2 μm and 0.8 nm, respectively. The oxygen content in the graphene is approximately 7 wt%. The synthesized processes of graphene are described below. Typically, graphite oxide (GO) was prepared from natural graphite through a modified Hummers method.[15] The GO was thermally treated at a high temperature under an N_2 flow and was then reduced at 1200 °C under an H_2 atmosphere.[16] To prepare graphene–cobalt oxide/cobalt composites, a hydrothermal method was used as reported previously.[17] In a typical synthesis, 0.2 g of $Co(NO_3)_2 \cdot 6H_2O$ was dissolved in 7 ml of distilled water under magnetic stirring. 0.005 g of graphene was dispersed in the solution under ultrasonic conditions, and 28 ml of 28–30% concentrated ammonia was slowly added. After sonication for 10 min, the mixture was transferred into a Teflon-lined stainless steel autoclave with a capacity of 50 ml for hydrothermal treatment at 100 °C for 8 h. As the autoclave cooled to room temperature naturally, the precipitates were separated by centrifugation, washed with distilled water and absolute ethanol, and dried under vacuum. Thus, a graphene–Co_3O_4 nanocomposite was obtained by annealing at 150 °C for 30 min under an Ar gas flow. After annealing at 270 °C for 1 h under an Ar/H_2 (10 vol%) gas flow, a graphene–Co nanocomposite was obtained.

Characterizations

XRD analyses were performed on an X'Pert Pro diffractometer with Cu Kα radiation ($\lambda = 1.54$ Å). Scanning electron microscopy (SEM) was performed on a scanning electron microscope (JEOL-JSM-6700F). High resolution scanning transmission electron microscopy (STEM) and electron energy loss spectroscopy (EELS) measurements were carried out on FEI Tecnai-F20 TEM operated at 200 kV.

Electrochemical measurements

A saturated calomel electrode (SCE) was used as the reference electrode in all measurements. Cyclic voltammetry (CV) and linear sweep voltammograms (LSVs) were conducted in a three-electrode electrochemical cell with a Pt plate (10 × 10 × 0.3 mm) and a glassy carbon (GC, $\varphi = 5$ mm) electrode as the counter electrode and the working electrode, respectively. The Pt/C (Hispec 3000, Alfa Aesar-A Johnson Matthey Company), cobalt(II,III) oxide (Co_3O_4, Strem Chemicals, Inc.), the pristine graphene, graphene–Co and graphene–Co_3O_4 catalysts were dispersed into a 1.0 mg ml^{-1} suspension with ethanol mixed with 0.05 wt% Nafion solution, respectively. Then 10 μl or 20 μl of the above suspensions was transferred onto the polished GC electrode substrates. The prepared electrodes were solidified for 0.5 hours under ambient conditions before testing. Electrochemical measurements were performed by CV with VMP3 (Bio-Logic SA) and a rotating disk electrode (RDE, M636, Pine Research Instrumentation). The scan rates were 100 mV s^{-1} for CV and 10 mV s^{-1} for ORR and OER measurements. All the potentials in LSV and CV measurements are relative to SCE.

The aqueous Li–air battery was assembled in a manner as that previously described.[3] The air catalytic electrode included a catalyst layer and a gas-diffusion layer. Teflon-treated carbon paper (Fuel Cell Store Inc., 200 μm in thickness) was used as the gas diffusion layer. Catalyst ink solutions were prepared by mixing the catalyst (80 wt%) with an ionomer (Tokuyama A4, 20 wt%) as a binder and tetrahydrofuran (Acros Organics) as a solvent in an ultrasonic bath for 1 h. The ink solution was sprayed onto one side of the Teflon-treated carbon paper. The area of the air electrode was 4 cm^2, and the mass loading of the catalyst sample was ~1.25 mg with a thickness of approximately 10 μm. The assembled Li–air battery was exposed to ambient air and connected to the testing station. A Solartron 1470 cell tester was employed to perform the charge and discharge tests at various current densities.

3. Results and discussion

The crystallinity and purity of the as-synthesized samples were investigated by X-ray powder diffraction (XRD). Fig. 1a shows a typical XRD pattern of the graphene–Co_3O_4 nanocomposite prepared under Ar atmosphere. In the XRD pattern, all diffraction peaks can be indexed to a cubic phase Co_3O_4 (JCPDS 43-1003). An additional small and broad diffraction peak that appears at 2θ of 22.5–27.5°, which can be indexed to the disordered graphene sheets, indicates that the composite consists of well-crystallized Co_3O_4 and disorderedly stacked graphene sheets. After the graphene–Co_3O_4 composite is annealed at 270 °C for 1 h under Ar–H_2 gas flow, the graphene–Co nanocomposite is obtained. Fig. 1b shows a typical XRD pattern that consists of the mixture of hexagonal phase cobalt (JCPDS 05-0727) and face-centered cubic phase cobalt (JCPDS 89-4307), which implies that the Co_3O_4 in the composite is transformed into the metallic cobalt after the thermal treatment in the Ar–H_2 gas flow. In addition, a weak diffraction hump at 2θ of 20–30° assigned to the graphene is still present in the pattern, suggesting that the nanocomposite consists of graphene and cobalt.

The size and morphology of the products were examined by SEM and TEM measurements. Low-magnification SEM and TEM images show that Co_3O_4 and Co nanoparticles are well

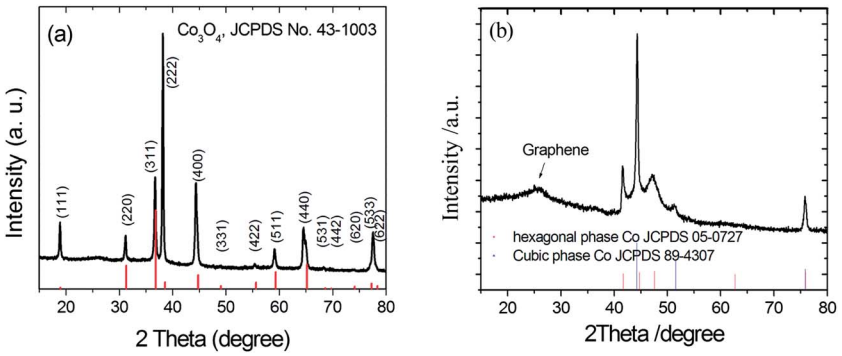

Fig. 1 XRD patterns of (a) the product synthesized under Ar atmosphere and (b) the product synthesized under H_2–Ar atmosphere.

dispersed on the surfaces of the graphene sheets. Fig. 2b and 3b show annular dark-field (ADF) scanning transmission electron microscopy (STEM) images of the as-prepared graphene–Co_3O_4 prepared under Ar and H_2–Ar atmospheres, respectively. The figures show that the Co_3O_4 particles have a diameter of approximately 200 nm and consist of numerous smaller NPs, forming a porous structure as shown in Fig. 2c. However, the Co nanoparticles have a similar size but with a solid structure (Fig. 3c), which indicates that the calcination atmosphere plays an import role in the morphology of the resultant products. Both the excellent conductive property of the graphene and the excellent catalytic properties of Co_3O_4 in addition to its porous characteristics, are expected to have favorable functions for ORR and OER.[18–21]

To further clarify the chemical composition of the samples obtained under different atmospheres, the electron energy-loss spectroscopy (EELS) results are shown in Fig. 2d and 3d, which reveal characteristic Co- and O-shell ionization edges. These results clearly indicate that nanoparticles on the graphene prepared under Ar and H_2–Ar atmospheres are Co_3O_4 and Co, respectively.

The ORR catalytic activities of the graphene–Co_3O_4 composites prepared under different atmospheres were studied by rotating disk electrode (RDE) in the O_2-saturated 0.1 M KOH solution and compared with those of the commercial Pt/C, commercial Co_3O_4 and the pristine graphene catalysts. Fig. 4a shows the cyclic voltammetry (CV) curves of the pristine graphene, commercial Co_3O_4 and the graphene–Co_3O_4 composite

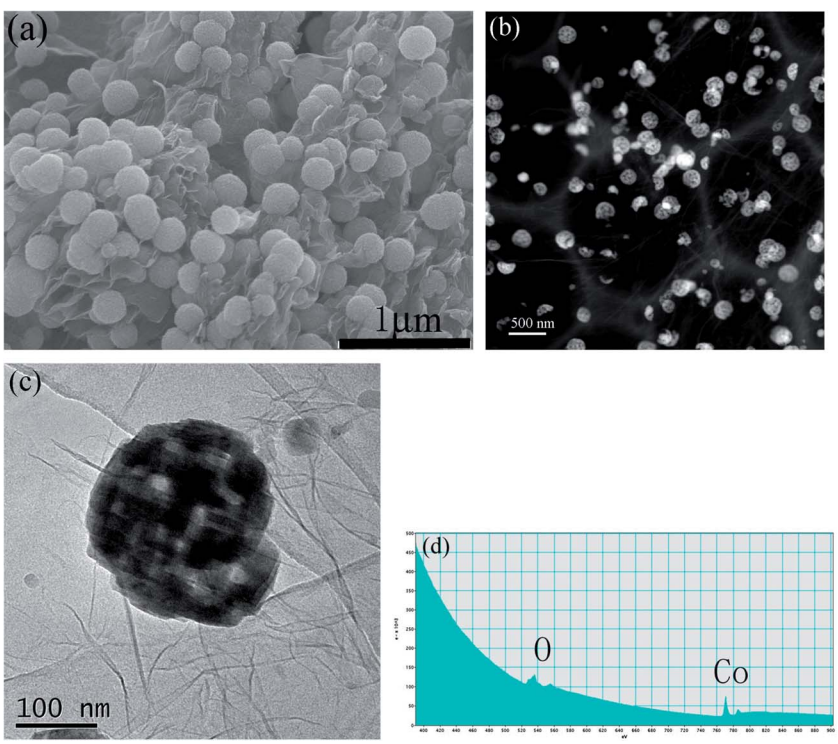

Fig. 2 (a) SEM, (b) ADF-STEM, and (c) TEM images of the as-prepared graphene–Co_3O_4 prepared under Ar atmosphere. (d) The corresponding EELS analysis obtained at the nanoparticle.

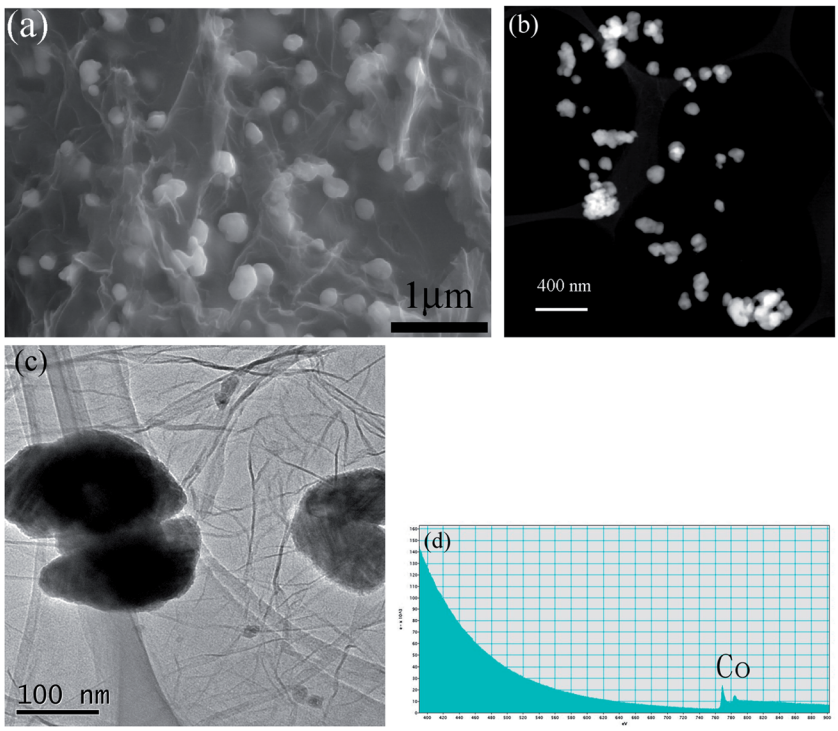

Fig. 3 (a) SEM, (b) ADF-STEM, and (c) TEM images of the as-prepared graphene–Co prepared under H_2–Ar atmosphere. (d) The corresponding EELS analysis obtained at the nanoparticle.

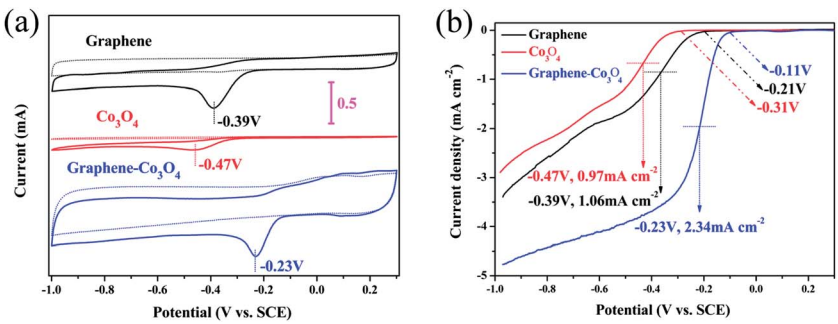

Fig. 4 Electrochemical ORR catalytic performance on different catalysts: (a) CV curves of the graphene–Co_3O_4 composite, the commercial Co_3O_4 and the pristine graphene on glassy carbon electrodes in O_2-saturated (solid line) or Ar-saturated 0.1 M KOH (dashed line) with a scan rate of 100 mV s^{-1} and (b) ORR polarization curves of different catalysts at a scan rate of 10 mV s^{-1} and a rotation speed of 1600 rpm in O_2-saturated 0.1 M KOH solution. Catalyst loading was 0.102 mg cm^{-2} for all catalysts.

in an O_2- or Ar-saturated 0.1 M KOH solution. Cathodic peaks are apparent in the O_2-saturated 0.1 M KOH solution, which are ascribed to the electrocatalytic oxygen reduction on the electrode. For fuel cells and metal–air batteries, an oxygen cathode with a high working potential leads to sufficiently high energy conversion efficiency. Therefore, it is important to compare the potential of oxygen reduction for different catalysts.[22,23] A better catalyst is characterized by a higher induced current density at a given applied potential or a more positive ORR onset potential. As shown in Fig. 4a, the graphene–Co_3O_4 composite shows considerably more positive ORR peak potential (~−0.23 V) than the pristine graphene and shows higher cathodic currents. Fig. 4b clearly shows the onset potential of the graphene–Co_3O_4 composite (~−0.11 V), which is higher than the pristine graphene (~−0.21 V) and the commercial Co_3O_4 (~−0.31 V). Alternatively, the half-wave potential, the potential at which the current is half of the limiting current in an LSV curve, has also been widely used for this purpose.[18] It is apparent in Fig. 4b that the current density of the graphene–Co_3O_4 composite at the half-wave potential is 2.34 mA cm^{-2}, which is about 2.41 and 2.21 times of that of the commercial Co_3O_4 (0.97 mA cm^{-2}) and the pristine graphene (1.06 mA cm^{-2}), respectively. Fig. S1a† shows the CV curve of the commercial Pt/C catalyst and compares it with that of the graphene–Co_3O_4 and graphene–Co. Fig. S1b† shows the ORR polarization curves obtained at a rotation rate of 1600 rpm. Both the positive potential and higher

current density suggest a synergetic effect in the graphene–Co_3O_4 catalyst for the ORR.

To gain more insight into the ORR process on the various catalysts, linear sweep voltammograms on an RDE were recorded at different rotating speeds from 400 rpm to 3600 rpm in 0.1 M KOH electrolyte saturated with O_2. It can be seen that the limiting current density increases with increasing rotation rate (Fig. 5a and c). The corresponding Koutecky–Levich (K–L) plots (Fig. 5b and d) show the inverse current (i^{-1}) as a function of the inverse of the square root of the rotation speed ($\omega^{-1/2}$) at different potential values. For comparison, Fig. S2a† shows LSVs of the commercial Pt/C catalyst at different rotating speeds. Fig. S2b† shows the K–L plots of the commercial Pt/C catalyst. The linearity of the K–L plots and near parallelism of the fitting lines at different potentials from −0.4 V to −0.9 V suggests first-order reaction kinetics toward the concentration of dissolved O_2 on various catalysts.[10] The number of electrons involved per O_2 in the ORR on various catalysts was determined by the Koutecky–Levich equation:[10]

$$\frac{1}{j} = \frac{1}{j_k} + \frac{1}{B\omega^{1/2}}, \quad (1)$$

where j_k is the kinetic current, ω is the angular velocity, and B is determined from the slope of the K–L plots based on the Levich equation as follows:

$$B = 0.62nF^{C_{O_2}}(D_{O_2})^{2/3}v^{-1/6}, \quad (2)$$

where n represents the number of electrons transferred per oxygen molecule (O_2), F is the Faraday constant (96 485 C mol^{-1}), D_{O_2} is the diffusion coefficient of O_2 in 0.1 M KOH (1.9×10^{-5} cm^2 s^{-1}), v is the kinetic viscosity (0.01 cm^2 s^{-1}), and C_{O_2} is the bulk concentration of O_2 (1.2×10^{-6} mol cm^{-3}).[12] The electron transfer number (n) in eqn (2) for the commercial Pt/C, graphene–Co_3O_4, and graphene–Co can be determined from the slopes of the K–L plots at −0.6 V to be about 4, 3.47 and 3.64, respectively. The calculated electron transfer numbers for the graphene–Co_3O_4, and graphene–Co are comparable to those of graphene-based catalysts,[12,23,24] which indicates the ORR on the graphene–Co_3O_4/Co catalysts favors a four-electron process.

Long-term stability of catalysts is an important parameter for their applications. To examine and compare the durability of the commercial Pt/C and graphene–Co_3O_4/Co prepared under different atmospheres, cyclic voltammetry was performed at a scan rate of 100 mV s^{-1} under ambient conditions. As shown in Fig. 6a, the solid lines and dashed lines correspond to the 1st and the 3000th scanning, respectively. After the 1st and 3000th CV scanning, the LSV curves of different catalysts were also recorded at a scan rate of 10 mV s^{-1} and a rotation speed of 1600 rpm in O_2-saturated 0.1 M KOH solution, shown in Fig. 6b–d. It can be seen clearly that the current densities were decreased with an increase in scanning time. Thus, the degradation rate was calculated by the following equation:

$$\text{Loss of current density } \% = (j_{1st} - j_{3000th})/j_{1st}, \quad (3)$$

where j_{1st} and j_{3000th} are the current density in the 1st and the 3000th LSV scanning at −0.2 V, respectively. The losses of current densities of the Pt/C, graphene–Co_3O_4, and graphene–Co catalysts were determined to be 48.8%, 46.5% and 50.6%, respectively. Therefore, graphene–Co_3O_4 shows better long-term stability than the Pt/C catalyst in an alkaline solution. It is widely accepted that the electrochemical corrosion of the carbon support is one of the most critical issues that affect the durability of the Pt/C catalyst.[25–30] These results indicate that

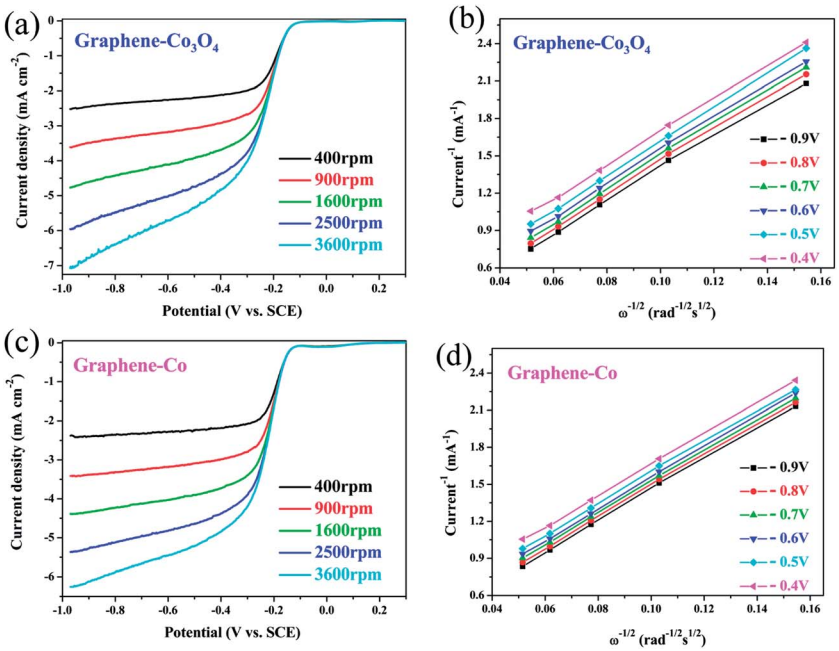

Fig. 5 LSVs at different rotating speeds and K–L plots of different catalysts at various potentials tested in O_2-saturated 0.1 M KOH: (a and b) graphene–Co_3O_4 catalyst; (c and d) graphene–Co catalyst.

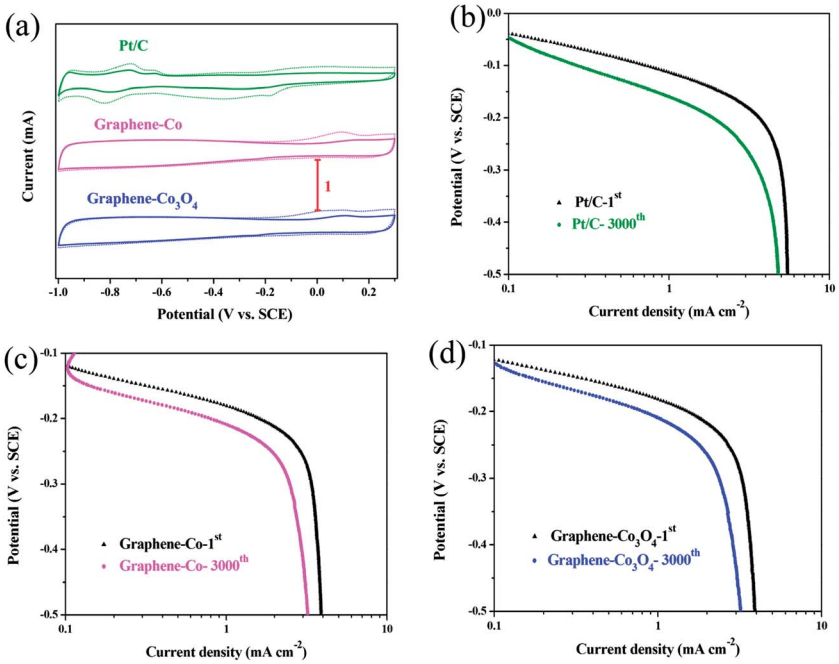

Fig. 6 Comparison of the long-term stability of Pt/C, graphene–Co_3O_4 and graphene–Co prepared under different atmospheres: (a) cyclic voltammetry scanned at a rate of 100 mV s^{-1} under ambient conditions; (b–d) LSV curves of different catalysts recorded at a scan rate of 10 mV s^{-1} and a rotation speed of 1600 rpm in an O_2-saturated 0.1 M KOH solution.

graphene-based composites have better corrosion-resistant performance in an alkaline solution.

To study the electrocatalytic activity of the catalysts for OER, LSV was performed with the pristine graphene, the commercial Co_3O_4 and the graphene–Co_3O_4 loaded on glassy carbon electrodes measured in an Ar-saturated 0.1 M KOH solution with a scan rate of 10 mV s^{-1}. As shown in Fig. 7a, the graphene–Co_3O_4, the pristine graphene, and the commercial Co_3O_4 catalysts resulted in a current density of 1.5 mA cm^{-2} at potentials of 0.65 V, 0.69 V and 0.73 V, respectively. Tafel plots of LSVs were derived and shown in Fig. 7b, from which small Tafel slopes down to 67.8, 69.1 and 71.4 mV per decade were found for the graphene–Co_3O_4, pristine graphene, and commercial Co_3O_4 catalysts, respectively. Similar to that of ORR, the graphene–Co_3O_4 also shows a synergetic effect for OER considering a decreased overpotential and a smaller Tafel slope.

For a rechargeable Li–air battery, a bifunctional electrocatalyst is required for simultaneously catalyzing ORR and OER reactions. In this work, we further examine the potential application of the graphene–Co_3O_4 catalyst in rechargeable Li–air batteries. The catalyst was tested in a cell with hybrid electrolytes as described in a previous study.[3] The first discharge and charge curves of the cell with the graphene–Co_3O_4 catalyst were compared with those tested with Vulcan XC-72 and state-of-the-art 50% Pt/C catalyst, as shown in Fig. 8a. The discharge voltage of the cells with the graphene–Co_3O_4 catalyst is lower than that of the 50% Pt/C catalyst but higher than that of the Vulcan XC-72 at the rate of 80 mA g^{-1}. It is obvious that the charge voltage of cells with the graphene–Co_3O_4 catalyst is lower than that of the Vulcan XC-72, which means that the graphene–Co_3O_4 catalyst is more effective for OER.

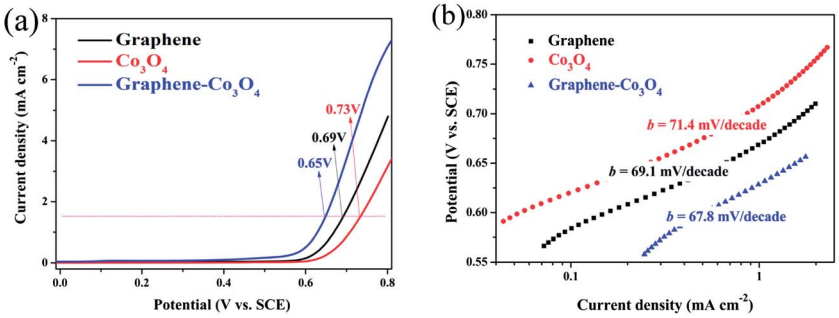

Fig. 7 (a) Oxygen evolution currents of the pristine graphene, the commercial Co_3O_4 and the graphene–Co_3O_4 on glassy carbon electrodes measured in an Ar-saturated 0.1 M KOH solution with a scan rate of 10 mV s^{-1}. (b) Tafel plots of OER currents in (a). Catalyst loading was 0.051 mg cm^{-2} for all the three catalysts.

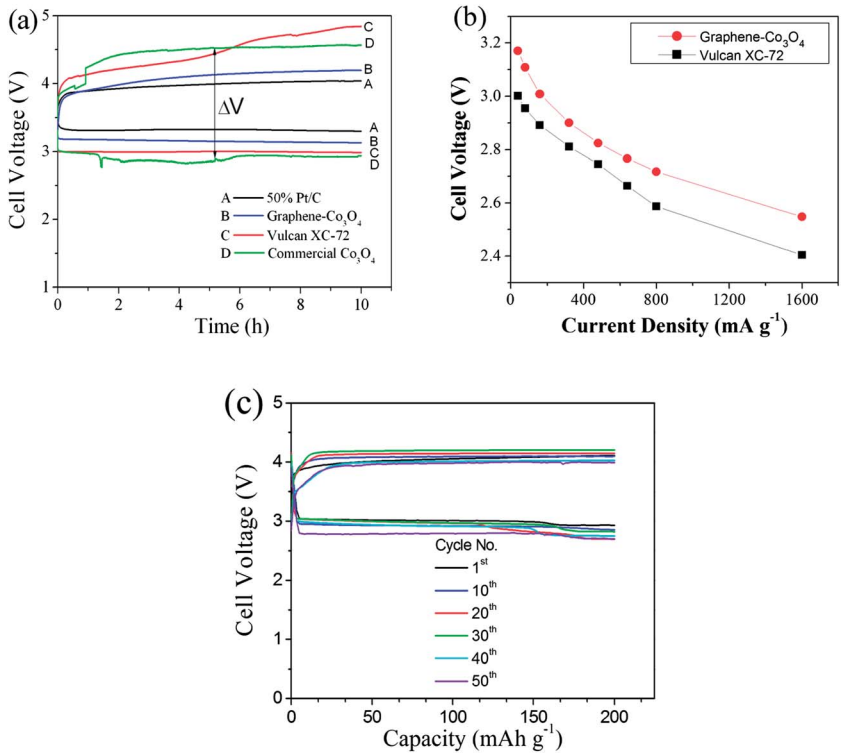

Fig. 8 (a) Comparison of the first charge and discharge curves of the prepared Li–air batteries with various catalysts at a current density of 80 mA g^{-1}. (b) Comparison of discharge voltage as a function of current density at different current densities shown by the Vulcan XC-72 and the graphene–Co_3O_4 catalyst. (c) Discharge–charge curves of the prepared Li–air batteries with the graphene–Co_3O_4 catalyst at a current density of 160 mA g^{-1} at different cycles. Catalyst loading was 1.25 mg.

The difference between discharge and charge voltages (ΔV) as marked in Fig. 8a for the Vulcan XC-72, commercial Co_3O_4 powder, graphene–Co_3O_4 and 50% Pt/C catalysts are 1.43 V, 1.65 V, 0.97 V and 0.68 V, respectively, at a current rate of 80 mA g^{-1}. The round-trip efficiency (the ratio of discharge to charge voltage) is 76.5% for the cell with the graphene–Co_3O_4 catalyst. This value is lower than that of the 50% Pt/C catalyst (83.0%) but higher than those of the Vulcan XC-72 (67.6%) and the commercial Co_3O_4 powder (63.8%). The discharge voltage of the commercial Co_3O_4 powder in micrometer size (Aldrich) is lower than that of the graphene–Co_3O_4, and the charge voltage is much higher (Fig. 8a). In addition, the graphene–Co_3O_4 operated well at high current rates (Fig. 8b). Fig. 8c shows the charge–discharge curves at a current density of 160 mA g^{-1}, which clearly indicate that the cell can be reversibly charged or discharged and that the graphene–Co_3O_4 catalyst has good cycle performance. It was reported in recent studies that Li–O_2 batteries tested with pure oxygen exhibited improved cycle performance with a larger capacity.[31] However, the electrochemical performances of the cell sharply degraded when tested under air atmosphere due to complex reactions arising from CO_2 and H_2O in air, as well as the clog effect of the discharged Li_2O_2 product in the porous electrode. In contrast to Li–O_2 batteries, our cell was exposed to air atmosphere during cycling of the cell, which was designed to test real air as the cathode for the Li–air battery. Although the recent Li–O_2 batteries with non-aqueous electrolytes showed relatively large capacities in the first cycle, they quickly degraded with cycling, even when tested under pure oxygen atmosphere.[32–34] It is worth noting that there is a limitation in solid electrolyte plate used for cell testing. The commercial solid electrolyte commonly used in an aqueous Li–air battery is $Li_{1+x+y}Al_xTi_{2-x}Si_yP_{3-y}O_{12}$ (OHARA Inc., Japan). This solid electrolyte has been known to be unstable in alkali liquid electrolytes for lengthy periods (>100 h), which eventually affects the cell voltage and cycle life.[35–37] Thus, the cycle test in this work was performed with a limited discharge–charge depth of 200 mA h g^{-1} and at a current rate of 160 mA g^{-1}. Considering the higher round-trip efficiency and excellent long-term stability as well as lower cost compared with noble metal catalysts, the graphene–Co_3O_4 material is a promising bifunctional catalyst for the Li–air battery.

4. Conclusion

In summary, we have successfully prepared a graphene–Co_3O_4 nanocomposite *via* a combined hydrothermal method and subsequent thermal treatment process. The obtained graphene–Co_3O_4 nanocomposite catalyst shows efficient and stable ORR and OER catalytic activities. More importantly, this catalyst shows a better long-term durability than the commercial Pt/C catalyst in an alkaline solution and may be used as an alternative to the commercial Pt/C catalyst for the ORR/OER in alkaline solutions. The improved performance of the graphene–Co_3O_4 nanocomposite catalyst can be ascribed to the synergetic effect

of Co_3O_4 and graphene. We believe that the present synthetic strategy can be extended to develop other 3D oxide/metal–graphene composites for various applications such as batteries, supercapacitors and sensors.

Author contributions

C.W.S. conceived and designed this work; C.W.S., Y.J.C., F.L. and Y.K. designed the experiments; Y.J.C. and Y.L.R. prepared the graphene–Co_3O_4/Co samples; C.M. and J.Q.L. performed TEM characterization; Y.J.C., W.Y. and Z.H.M. carried out the SEM and XRD characterizations; F.L. and Y.W. performed CV and LSV tests; and Y.K. tested the Li–air batteries. All the authors participated in the analysis and discussions of the results and in preparing the manuscript.

Acknowledgements

This work is financially supported by the National Science Foundation of China (NSFC) (Grant no. 51372271, 51172275, 51172007, 11004229), the National Key Basic Research Program of China (Grant No. 2012CB215402) and a start up grant from Institute of Physics (IOP). Y. Chen's work is supported by the National Natural Science Fund of China (Grant no. 51272050) and Program for New Century Excellent Talents in University (NECT-10-0049). Y. Kim's work was supported by the 2013 Research Fund (1,130064,01) of UNIST (Ulsan National Institute of Science and Technology).

References

1 B. Lim, M. Jiang, P. H. C. Camargo, E. C. Cho, J. Tao, X. Lu, Y. Zhu and Y. Xia, Pd–Pt bimetallic nanodendrites with highly activity for oxygen reduction, *Science*, 2009, **324**, 1302–1305.

2 C. Sun, R. Hui and J. Roller, Cathode materials for solid oxide fuel cells: A review, *J. Solid State Electrochem.*, 2010, **14**, 1125–1144.

3 W. Yang, J. Salim, S. Li, C. Sun, L. Chen, J. B. Goodenough and Y. Kim, Perovskite $Sr_{0.95}Ce_{0.05}CoO_{3-\delta}$ loaded with copper nanoparticles as a bifunctional catalyst for lithium–air batteries, *J. Mater. Chem.*, 2012, **22**, 18902–18907.

4 W. Yang, J. Salim, C. Ma, Z. Ma, C. Sun, J. Li, L. Chen and Y. Kim, Flowerlike Co_3O_4 microspheres loaded with copper nanoparticles as an efficient bifunctional catalyst for lithium–air batteries, *Electrochem. Commun.*, 2013, **28**, 13–16.

5 A. Christensen, P. Albertus, R. S. Sanchez-Carrera, T. Lohmann, B. Kozinsky, R. Liedtke, J. Ahmed and A. Kojic, A Critical Review of Li/Air Batteries, *J. Electrochem. Soc.*, 2012, **159**, R1–R30.

6 Y. Lu, Z. Xu, H. A. Gasteiger, S. Chen, K. Hamad-Schifferli and S. H. Yang, Platinum–gold nanoparticles: a highly active bifunctional electrocatalyst for rechargeable lithium–air batteries, *J. Am. Chem. Soc.*, 2010, **132**, 12170–12171.

7 M. Hamdani, R. N. Singh and P. Chartier, Co_3O_4 and Co-based spinel oxides bifunctional oxygen electrodes, *Int. J. Electrochem. Sci.*, 2010, **5**, 556–577.

8 J. Xu, P. Gao and T. S. Zhao, Non-precious Co_3O_4 nano-rod electrocatalyst for oxygen reduction in anion-exchange membrane fuel cells, *Energy Environ. Sci.*, 2012, **5**, 5333–5339.

9 A. Débart, J. Bao, G. Armstrong and P. G. Bruce, An O_2 cathode for rechargeable lithium batteries: the effect of a catalyst, *J. Power Sources*, 2007, **174**, 1177–1182.

10 Y. Liang, Y. Li, H. Wang, J. Zhou, J. Wang, T. Regier and H. Dai, Co_3O_4 nanocrystals on graphene as a synergistic catalyst for oxygen reduction reaction, *Nat. Mater.*, 2011, **10**, 780–786.

11 S. Yang, L. Zhi, K. Tang, X. Feng, J. Maier and K. Müllen, Efficient synthesis of heteroatom (N or S)-doped graphene based on ultrathin graphene oxide-porous silica sheets for oxygen reduction reactions, *Adv. Funct. Mater.*, 2012, **22**, 3634–3640.

12 J. Liang, Y. Jiao, M. Jaroniec and S. Z. Qiao, Sulfur and nitrogen dual-doped mesoporous graphene electrocatalyst for oxygen reduction with synergistically enhanced performance, *Angew. Chem., Int. Ed.*, 2012, **51**, 11496–11500.

13 W. Ryu, T. Yoon, S. H. Song, S. Jeon, Y. Park and I. Kim, Bifunctional composite catalysts using Co_3O_4 nanofibers immobilized on nonoxidized graphene nanoflakes for high-capacity and long-cycle Li–O_2 batteries, *Nano Lett.*, 2013, **13**, 4190–4197.

14 H. Lim, H. Gwon, H. Kim, S. Kim, T. Yoon, J. W. Choi, S. M. Oh and K. Kang, Mechanism of Co_3O_4/grapheme catalytic activity in Li–O_2 batteries using carbonate based electrolyte, *Electrochim. Acta*, 2013, **90**, 63–70.

15 W. S. Hummers and R. E. Offeman, Preparation of graphitic oxide, *J. Am. Chem. Soc.*, 1958, **80**, 1339.

16 Y. Ren, C. Zhu, S. Zhang, C. Li, Y. Chen, P. Gao, P. Yang and Q. Ouyang, Three-dimensional SiO_2@Fe_3O_4 core/shell nanorod array/graphene architecture: synthesis and electromagnetic absorption properties, *Nanoscale*, 2013, **5**, 12296–12303.

17 Y. Chen, Q. Wang, C. Zhu, P. Gao, Q. Ouyang, T. Wang, Y. Ma and C. Sun, Graphene/porous cobalt nanocomposite and its noticeable electrochemical hydrogen storage ability at room temperature, *J. Mater. Chem.*, 2012, **22**, 5924–5927.

18 L. Su, Y. Jing and Z. Zhou, Li ion battery materials with core–shell nanostructures, *Nanoscale*, 2011, **3**, 3967–3983.

19 M. Yang, J. X. Li, H. H. Li, L. W. Su, J. P. Wei and Z. Zhou, Mesoporous slit-structured NiO for high-performance pseudocapacitors, *Phys. Chem. Chem. Phys.*, 2012, **14**, 11048–11052.

20 S. M. Yuan, J. X. Li, L. T. Yang, L. W. Su, L. Liu and Z. Zhou, Preparation and lithium storage performances of mesoporous Fe_3O_4@C microcapsules, *ACS Appl. Mater. Interfaces*, 2011, **3**, 705–709.

21 Z. Zhang, L. Su, M. Yang, M. Hu, J. Bao, J. Wei and Z. Zhou, A composite of Co nanoparticles highly dispersed on N-rich carbon substrates: an efficient electrocatalyst for Li–O_2 battery cathodes, *Chem. Commun.*, 2014, **50**, 776–778.

22 S. Wang, L. Zhang, Z. Xia, A. Roy, D. W. Chang, J. Baek and L. Dai, BCN graphene as efficient metal-free electrode

catalyst for the oxygen reduction reaction, *Angew. Chem., Int. Ed.*, 2012, **51**, 4209–4212.

23 S. Guo, S. Zhang, L. Wu and S. Sun, Co/CoO nanoparticles assembled on graphene for electrochemical reduction of oxygen, *Angew. Chem., Int. Ed.*, 2012, **51**, 11770–11773.

24 Z. Liu, G. Zhang, X. Jin, Z. Chang and X. Sun, One-step scalable preparation of N-doped nanoporous carbon as high-performance electrocatalysts for oxygen reduction reaction, *Nano Res.*, 2013, **6**, 293–301.

25 L. M. Roen, C. H. Paik and T. D. Jarvi, Electrocatalytic corrosion of carbon support in PEMFC cathodes, *Electrochem. Solid-State Lett.*, 2004, **7**, A19–A22.

26 E. Antolini, Formation, microstructural characteristics and stability of carbon supported platinum catalysts for low temperature fuel cells, *J. Mater. Sci.*, 2003, **38**, 2995–3005.

27 K. H. Kangasniemi, D. A. Condit and T. D. Jarvi, Characterization of Vulcan Electrochemically oxidized under simulated PEM fuel cell conditions, *J. Electrochem. Soc.*, 2004, **151**, E125–E132.

28 X. Wang, W. Li, Z. Chen, M. Waje and Y. Yan, Durability investigation of carbon nanotube as catalyst support for proton exchange membrane fuel cell, *J. Power Sources*, 2006, **158**, 154–159.

29 Y. Shao, G. Yin, Y. Gao and P. Shi, Durability Study of Pt/C and Pt/CNTs Catalysts under Simulated PEM Fuel Cell Conditions, *J. Electrochem. Soc.*, 2006, **153**, A1093–A1097.

30 R. Borup, J. Meyers, B. Pivovar, Y. S. Kim, R. Mukundan, N. Garland, D. Myers, M. Wilson, F. Garzon, D. Wood, P. Zelenay, K. More, K. Stroh, T. Zawodzinski, J. Boncella, J. E. McGrath, M. Inaba, K. Miyatake, M. Hori, K. Ota, Z. Ogumi, S. Miyata, A. Nishikata, Z. Siroma, Y. Uchimoto, K. Yasuda, K. I. Kimijima and N. Iwashita, Scientific aspects of polymer electrolyte fuel cell durability and degradation, *Chem. Rev.*, 2007, **107**, 3904–3951.

31 D. Xu, Z. L. Wang, J. J. Xu, L. L. Zhang, L. M. Wang and X. B. Zhang, A stable sulfone based electrolyte for high performance rechargeable Li–O_2 batteries, *Chem. Commun.*, 2012, **48**, 11674–11676.

32 Y. Yu, B. Zhang, Y. He, Z. Huang, S. Oh and J. Kim, Mechanisms of capacity degradation in reduced grapheme oxide/α-MnO_2 nanorod composite cathodes of Li–air batteries, *J. Mater. Chem. A*, 2013, **1**, 1163–1170.

33 K. Guo, Y. Li, J. Yang, Z. Zou, X. Xue, X. Li and H. Yang, Nanosized Mn–Ru binary oxides as effective bifunctional cathode electrocatalysts for rechargeable Li–O_2 batteries, *J. Mater. Chem. A*, 2014, **2**, 1509–1514.

34 L. Xu, J. Ma, B. Li and F. Kang, A novel air electrode design: A key to high rate capability and long life span, *J. Power Sources*, 2014, **255**, 187–196.

35 S. Hasegawa, N. Imanishi, T. Zhang, J. Xie, A. Hirano, Y. Takeda and O. Yamamoto, Study on lithium/air secondary batteries-stability of NASICON-type lithium ion conducting glass–ceramic with water, *J. Power Sources*, 2009, **189**, 371–377.

36 T. Zhang, N. Imanishi, Y. Shimonishe, A. Hirano, J. Xie, Y. Takeda, O. Yamamoto and N. Sammes, Stability of a water-stable lithium metal anode for a lithium–air battery with acetic acid–water solutions, *J. Electrochem. Soc.*, 2010, **157**, A214–A218.

37 T. Zhang, N. Imanishi, Y. Takeda and O. Yamamoto, Aqueous lithium/air rechargeable batteries, *Chem. Lett.*, 2011, **40**, 668–673.

